# TOPOLOGY OPTIMIZATION OF COUPLED THERMOMECHANICAL ANALYSIS FOR ADDITIVE MANUFACTURING

Jack S. Ramsey, Dr. Douglas E. Smith

Baylor University
Waco, Texas

## ABSTRACT

Topology optimization methods have been developed over the past three decades to optimize the structural design of composite parts. It is now possible to fabricate complex  structures generated from topology optimization with additive manufacturing techniques such as large-scale polymer composite deposition. However, large-scale polymer composite deposition produces strutures with anisotropic material properties. This directional orienation affects the structural response of the part and the structure's behavior during the printing process where thermal stress can led to unacceptable distortion. This paper presents a topology optimization approach that considers the structural response of the product during its use and the printing process employed in its manufacturing. A finite element-based topology optimization algorithm is developed to model structures under weakly coupled thermomechanical loads and anisotropic material properties. Design derivatives are evaluated using the adjoint variable method for the weakly coupled thermal-mechanical system. An optimality criterion-based algorithm maximizes the stiffness of a two-dimensional design space over material density and direction. We consider a steady-state thermal response where the resulting thermal stresses are included in the mechanical optimization. This weakly coupled thermal analysis and material direction optimization includes the anisotropic Young's modulus and thermal stresses present in large-scale polymer deposition and extends topology optimization to weakly coupled thermomechanical systems with design-dependent temperature fields.  Examples are given to demonstrate our proposed weakly coupled system topology optimization.

## 1. INTRODUCTION

Additive manufacturing (AM) has moved from a rapid-prototyping method to a robust manufacturing technique in the past several years and allows for unprecedented design flexibility. However, several factors specific to the fabrication process, such as thermal warping and anisotropic material properties, pose a challenge to part design and fabrication.

Topology optimization, a structural optimization method that determines the material distribution for a structure that optimizes an important response such as compliance or strain energy. The resulting structures are often complex enough that only additive manufacturing can feasibly produce the parts. Existing topology optimization methods have been applied to yield novel AM structures, but have yet to consider the fabrication challenges unique to additive manufacturing such as non-isothermal conditions during printing. In addition, print beads produced with AM polymer deposition processes are known to be non-isotropic due to highly orientated microstructures in the printed bead.

The topology optimization algorithm presented here optimizes the design of a two-dimensional part under weakly coupled steady state thermomechanical loading and anisotropic spatially varying material properties. Our approach includes material anisotropy and temperature-induced stresses in additive manufacturing and is a step toward modeling transient heat transfer.

The algorithm presented here is developed to optimize either the compliance or strain energy of a two-dimensional design space over both material density and direction. Our approach models the weakly coupled thermomechanical system and uses the optimality criteria method to solve the constrained minimization problem. The compliance and strain energy design sensitivities are derived and applied through a custom Matlab-based two-dimensional finite element program. Optimized designs for numerous thermomechanical systems are obtained for both compliance and strain energy minimization, and their performance is compared. It is shown that the proposed topology optimization algorithm can produce printable proof-of-concept optimized parts.

## 1.1 Topology Optimization Background

Topology optimization is a structural optimization method that was introduced by Bendsoe and Kikuchi in 1988 [1] to determine the optimal design for mechanical parts. Their homogenization update scheme has been joined by the method of moving asymptotes [2], the optimality criterion method [3], the level-set method [4], and many other techniques. Topology optimization has been applied to structures with multiple loading conditions and heat transfer problems, and have included fundamental frequency of vibration, multiphase materials, anisotropic materials, compliant mechanisms, and piezoelectric actuators. See the text by Bendsoe and Sigmund [5] for these and other topology optimization examples.

The anisotropic nature of additively manufactured materials can be optimized in topology optimization. More recently, Hoglund [6] developed a topology optimization approach for AM structures composed of anisotropic materials, which was later extended by Jiang [7] to three dimensional structures with elastic non-isotropic properties derived specifically for large scale AM polymer deposition. Their use of a general nonlinear programming algorithm as in [8] instead of the commonly used optimality criteria, a topology optimization-specific update scheme (see [3]) increased the computational burden but demonstrated that optimizing the fiber direction is feasible. A similar approach was employed by Drs. Luo and Gea [9].

Despite the application of topology optimization to problems governed by various disciplines, to the best of our knowledge, there has yet to be a rigorous development of the method for non-isothermal thermomechanical systems. Dr. Deaton [10] considered constant-temperature thermomechanical topology optimization for aircraft fuselages. Pederson and Pederson [11] suggested alternatives to optimizing compliance, as it does not always maximize strength. Zhang, et al, [12] proposed strain energy as an alternative for compliance and demonstrated that parts optimized for strain energy can have lower maximum stress than parts optimized for strain energy. Drs. Neiford, et. al, used the level-set method to compare compliance and strain energy minimization for isothermal thermomechanical systems [13].

In summary, anisotropic material has been considered for topology optimization, but only in the context of pure mechanical loads, and the existing methods are robust but computationally complex. Weakly coupled thermomechanical systems, where a temperature field creates thermal stresses that affect the mechanical displacements, have only been modeled for constant temperature. While the step from fixed temperature to design-dependent temperature seems minimal, it can introduce stability issues that prevent convergence of the topology optimization algorithm, which have been explored in our current work.

### 1.2 Additive Manufacturing Developments

The structures derived from topology optimization are frequently complex, and additive manufacturing is often the only feasible manufacturing method. The development of additive manufacturing from a prototyping method to a rapidly growing manufacturing method is now enabling the production and use of topology optimized parts.

Big-area additive manufacturing is of interest for topology optimization of large structural parts. Oak Ridge National Laboratory and Cincinnati Incorporated developed the first industrial-sized fiber-reinforced composite printer. It has been used to print several large objects, like a car chassis, wind turbine blade molds, and a yacht mold, out of carbon fiber-filled ABS. The drastic increase in scale over standard tabletop-sized fused-filament fabrication printers opens new areas for manufacturing. An explanation of the method, challenges, and some simulation methods can be found in [14]. Oak Ridge National Laboratory has proposed a one-dimensional cooling model for big-area additive manufacturing [15], which can be used to predict thermal stresses.

### 1.3 Manufacturing Challenges in Additive Manufacturing

Polymer composite additive manufacturing systems produce parts with highly anisotropic material properties. The polymer molecules tend to become aligned in the bead direction as they are extruded, and air pockets between adjacent beads contribute to the anisotropy. Further, as each layer of polymer cools after extrusion, bonding between layers becomes weaker. Printed parts usually have a much weaker stiffness and strength in the direction perpendicular to the build plane and are weaker where beads meet. The latter can be mitigated somewhat by alternating the bead direction in different layers, so that the stiffness is still weaker but not as directionally dependent, but the former still causes significant anisotropy.

Some of the weakness can be countered by adding fibers to the polymer. Adding small chopped glass fiber or carbon fiber increases the stiffness of the composite, but the fibers tend to align along the bead direction during extrusion and increase the anisotropy. The increased stiffness can improve part performance, but the anisotropy must be modeled adequately.

Adding fibers also counters the thermal stresses that can weaken or warp parts. As the polymer cools from the molten extrusion state, it contracts. The next layer laid down on top cools and contracts again, and several layers of this can cause deformation perpendicular to the build plane. The lower coefficient of thermal expansion of the fibers dampens this effect but does not eliminate it. Further, even when no deformations are visible, this cooling can create thermal stresses in the part. Depending on the loading case, these can increase or decrease stiffness and must be considered.

Thus, modeling additive manufacturing involves precisely the challenges that topology optimization is now beginning to address. The necessary steps include optimizing material location and orientation simultaneously to model fiber-reinforced polymer and extending the modeling to include weakly coupled thermomechanical systems to model thermal stresses. An algorithm has been developed below that optimizes both compliance and strain energy for these conditions.

# 2. EXPERIMENTATION

## 2.1 Finite Element Formulation

The topology optimization considered in this paper is solved on a two-dimensional domain that is discretized into square linear finite elements. Governing partial differential equations for both two-dimensional linear thermal conduction and elasticity are defined over the domain and are each transformed into linear finite element matrix equations in the usual manner. We consider that the thermal conduction system relates a cooling process that occurs as part of the material processing step during part manufacturing (i.e., cooling following polymer composite extrusion) and the mechanical system represents the loaded part during its use. Note that the steady-state thermal loading developed here does not represent the complexity that a part might experience during polymer extrusion additive manufacturing, however, we consider that this is a first step toward modeling the full process.

Following common finite element procedures, the discretized algebraic equations may be written in terms of the element thermal system matrices $K_{Th_i}$ which are defined in terms of the *i*-th element topology optimization design variable $x_i$ as

$$K_{Th_i} = x_i^p \int_{V_i} B_{Th}^T D_{Th} B_{Th} dV_i \tag{1}$$

where the subscript *Th* indicates the thermal problem; and $p$ is a penalty parameter used in the topology optimization algorithm described below, $B_{Th}$ is the temperature gradient matrix, $D_{Th}$is the isotropic elasticity matrix, and $V_i$ is the volume of the *i*-th element. Here, $x_i$ represents the density of the $i$-th element.

In a similar manner, the governing differential equation for linear elasticity problem yields matrix equations written in terms of the element he stiffness matrix for the *i*-th element as

$$K_{M_i} = x_i^p \int_{V_i} B_M^T R^T(\theta_i) D_M R(\theta_i) B_M dV_i \tag{2}$$

which assumes an anisotropic material response defined in terms of the angle $\theta_i$. In the above, the subscript *M* indicates the mechanical simulation and the displacement gradient matrix $B_M$ is from the weak form of the elastic governing equations. The anisotropic elasticity matrix $D_M$ and the rotation matrix $R(\theta_i)$ are written respectively as

$$D_M = \begin{bmatrix} \frac{E_x}{1-\nu_{xy}\nu_{yx}} & \frac{\nu_{xy}E_y}{1-\nu_{xy}\nu_{yx}} & 0 \\ \frac{\nu_{xy}E_y}{1-\nu_{xy}\nu_{yx}} & \frac{E_y}{1-\nu_{xy}\nu_{yx}} & 0 \\ 0 & 0 & G_{xy} \end{bmatrix} \tag{3}$$

and

$$R(\theta_i) = \begin{bmatrix} cos^2(\theta_i) & sin^2(\theta_i) & -2 * sin(\theta_i) * cos(\theta_i) \\ sin^2(\theta_i) & cos^2(\theta_i) & 2 * sin(\theta_i) * cos(\theta_i) \\ sin(\theta_i) * cos(\theta_i) & -sin(\theta_i) * cos(\theta_i) & cos^2(\theta_i) - sin^2(\theta_i) \end{bmatrix} \tag{4}$$

The thermal finite element equations are solved first to obtain nodal temperatures which are then used to compute the thermal loads on the *i*-th element for the mechanical model as

$$F_{Th_i} = x_i^p \int_{V_i} B_M^T D_M \begin{Bmatrix} \alpha \\ \alpha \\ 0 \end{Bmatrix} N_i^T T_i dV_i \tag{5}$$

where $T_i$ and $N_i$ are the nodal temperature vector and shape function vector, respectively, for the $i$-th element. Thermal loads computed from Equation (5) serve as input to the mechanical model in the usual manner. The global finite element equations satisfy the equilibriums $K_{Th}T = F_{TF}$, $KU = F$, and $KU_{Th} = F_{Th}$, where $T$ is the global temperature vector, $F_{TF}$ is the global heat flux vector, $U$ is the global displacement vector, $F$ is the global force vector, $U_{Th}$ is the global vector of displacements due to thermal forces, and $F_{Th}$ is the global vector of thermal loads.

## 2.2 Optimality Criteria Update

The topology optimization method treats the element densities $x_i$ and angles $\theta_i$ as design variables and seeks to minimize a given function subject to a volume constraint.

$$minimize\ f(x, \theta) \tag{6}$$

$$subject\ to\ \frac{\sum x_i}{N_{el}} \le V_f$$

where $N_{el}$ is the number of elements in the finite element discretization. The algorithm iterates by updating the density according to one of many heuristic schemes so that the volume constraint is satisfied at each iteration. The iterations continue until the maximum change in the density of the elements is below some threshold.

The densities $x_i \in [x_{min}, 1]$ represent the amount of material in each element, and it is desired that each density is $x_{min}$ or 1 at the end of the simulation. This indicates that either material is present ($x_i = 1$) or no material is present ($x_i = x_{min}$) at each element. Note that the minimum density $x_{min} > 0$ is chosen to be small but nonzero to avoid singularities in the finite element method.

It is typical to use compliance as the objective function in the topology optimization problem, however, we also consider strain energy as an alternate objective. Compliance *C* and strain energy *S* are respectively defined as

$$C = U^T F \tag{7}$$

and

$$S = \frac{1}{2} U^T F - U^T F_{Th} + \frac{1}{2} U_{Th}^T F_{Th} \tag{8}$$

In the optimality criteria method for the topology optimization algorithm, the element densities $x_i$ are updated according to

$$x_i^{new} = \begin{cases} max(x_{min}, x_i - m), & if\ x_i B_i^{\eta} \leq max(x_{min}, x_i - m) \\ min(1, x_i + m), & if\ x_i B_i^{\eta} \geq min(1, x_i + m) \\ x_i B_i^{\eta}, & else \end{cases} \tag{9}$$

where

$$B_i = \frac{\frac{-df}{dx_i}}{\lambda} \tag{10}$$

Here *F* is the objective function which is either compliance *C* or strain energy *S* in the examples below. In equation (5), the Lagrange multiplier $\lambda$ is found via a bisection algorithm to preserve the global volume constraint as in Sigmund [8]. The move limit $m = 0.2$ is set to prevent wide swings in density. The damping coefficient $\eta = 0.5$ is likewise chosen to help stabilize the iterative procedure. Both are tunable parameters which contribute to the stability of the algorithm.

Once the element densities have been updated, the element angles are updated. For each element $i$, the angle $\theta_{i_{min}}$ that minimizes the objective function over $V_i$ is found for the local displacements $U_i$, which are fixed for this step, and the element mechanical stiffness $K_{M_i}$. The angle is then updated according to:

$$\theta_i = \begin{cases} \max(\theta_i - L, 0), & \theta_{i_{min}} < \theta_i - L \\ \theta_{i_{min}}, & abs(\theta_{i_{min}} - \theta_i) \leq L \\ \min(\theta_i + L, 2\pi), & \theta_{i_{min}} > \theta_i + L \end{cases} \tag{11}$$

### 2.3 Design Sensitivity Derivation

The optimality criteria method described above updates element density design variables using Equation (10) which requires design sensitivities $\frac{df}{dx_i}$. We derive expressions for the $\frac{df}{dx_i}$ using the adjoint method which are then evaluated with the finite element method. We first consider the sensitivity of compliance defined in Equation (7) with respect to an element design variable xi by defining an augmented functional $\hat{C}$ for compliance written in terms of the mechanical system's Lagrange multiplier vector $\lambda$ as

$$\hat{C} = C - \lambda(KU - F) \tag{12}$$

The design derivative of $\hat{C}$ with respect to the i-th element density xi is

$$\frac{d\hat{C}}{dx_i} = \frac{d}{dx_i}(C) - \lambda\frac{d}{dx_i}(KU - F) = \frac{\partial C}{\partial U}\frac{dU}{dx_i} + \frac{\partial C}{\partial F}\frac{dF}{Dd} - \lambda(\frac{dK}{dx_i}U + K\frac{dU}{dx_i} - \frac{dF}{dx_i})$$

$$\frac{d\hat{C}}{dx_i} = \left(\frac{\partial C}{\partial U} - \lambda K\right)\frac{dU}{dx_i} + \left(\frac{\partial C}{\partial F} + \lambda\right)\frac{dF}{dx_i} - \lambda\frac{dK}{dx_i}U$$

$$\frac{d\hat{C}}{dx_i} = (F - \lambda K)\frac{dU}{dx_i} + (U^T + \lambda)\frac{dF}{dx_i} - \lambda\frac{dK}{dx_i}U \tag{13}$$

In the adjoint problem for compliance, it is easy to show that $\lambda = U^T$ which may be substituted into Equation (13) to yield

$$\frac{d\hat{C}}{dx_i} = 2U^T\frac{dF}{dx_i} - U^T\frac{dK}{dx_i}U = 2U^T\left(\frac{\partial F}{\partial x_i} + \frac{\partial F}{\partial T}\frac{dT}{dx_i}\right) - U^T\frac{dK}{dx_i}U$$

From the thermal equilibrium finite element equation, $K_tT = F_t$, so $\frac{dK_t}{dx_i}T + K_t\frac{dT}{dx_i} = \frac{dF_t}{dx_i} = 0$ and $\frac{dT}{dx_i} = -K_t^{-1}\frac{dK_t}{dx_i}T$ which yields

$$\frac{d\hat{C}}{dx_i} = 2U^T\left(\frac{\partial F}{\partial x_i} - \frac{\partial F}{\partial T}K_t^{-1}\frac{dK_t}{dx_i}T\right) - U^T\frac{dK}{dx_i}U \tag{14}$$

and

$$\frac{d\hat{C}}{dx_i} = -px_i^{p-1}U_i^TK_iU_i + 2U_i^T\frac{\partial F_{th}}{\partial x_i} - 2px_i^{p-1}\left(\frac{\partial F_{th}}{\partial T}K_t^{-1}\right)_i K_{t_i}T_i \tag{15}$$

When strain energy S is used to define the topology optimization objective function, we obtain the design sensitivities in a similar manner by first defining an augmented functional $\hat{S}$ in terms of the mechanical and thermal Lagrange multipliers, $\lambda$ and $\gamma$, respectively, written as

$$\hat{S} = S - \lambda(KU - F) - \gamma(KU_{th} - F_{th}) \tag{16}$$

The derivative of $\hat{S}$ with respect to the element density xi is

$$\frac{d\hat{S}}{dx_i} = \frac{dS}{dx_i} - \lambda\frac{d}{dx_i}(KU - F) - \gamma(KU_{th} - F_{th})$$

which is written in terms of the related finite element matrices as

$$\frac{d\hat{S}}{dx_i}=\frac{\partial S}{\partial U}\frac{dU}{dx_i}+\frac{\partial S}{\partial F}\frac{dF}{dx_i}+\frac{\partial S}{\partial U_{th}}\frac{dU_{th}}{dx_i}+\frac{\partial S}{\partial F_{th}}\frac{dF_{th}}{dx_i}-\lambda\left(\frac{dK}{dx_i}U+K\frac{dU}{dx_i}-\frac{dF}{dx_i}\right)-\gamma(\frac{dK}{dx_i}U+K\frac{dU_{th}}{dx_i}-\frac{dF_{th}}{dx_i})$$

or

$$\frac{d\hat{S}}{dx_i}=\left(\frac{\partial S}{\partial U}-\lambda K\right)\frac{dU}{dx_i}+\left(\frac{\partial S}{\partial U_{th}}-\gamma K\right)\frac{dU_{th}}{dx_i}+\left(\frac{\partial S}{\partial F}+\lambda\right)\frac{dF}{dx_i}+\left(\frac{\partial S}{\partial F_{th}}+\gamma\right)\frac{dF_{th}}{dx_i}-\lambda\frac{dK}{dx_i}U-\gamma\frac{dK}{dx_i}U_{th}$$

After some algebraic manipulations, we obtain

$$\frac{d\hat{S}}{dx_i}=\left(\frac{1}{2}F-F_{th}-\lambda K\right)\frac{dU}{dx_i}+\left(\frac{1}{2}F_{th}-\gamma K\right)\frac{dU_{th}}{dx_i}+\left(\frac{1}{2}U^T+\lambda\right)\frac{dF}{dx_i}+\left(-U^T+\frac{1}{2}U_{th}+\gamma\right)\frac{dF_{th}}{dx_i}-\lambda\frac{dK}{dx_i}U-\gamma\frac{dK}{dx_i}U_{th} \tag{17}$$

Solution to the related adjoint variable problems yield $\lambda=\frac{1}{2}U^T-U_{th}^T$ and $\gamma=\frac{1}{2}U_{th}^T$. which are substituted into Equation (17) to obtain

$$\frac{d\hat{S}}{dx_i}=\left(\frac{1}{2}U^T+\frac{1}{2}U^T-U_{th}^T\right)\frac{dF}{dx_i}+\left(-U^T+\frac{1}{2}U_{th}+\frac{1}{2}U_{th}^T\right)\frac{dF_{th}}{dx_i}-(\frac{1}{2}U^T-U_{th}^T)\frac{dK}{dx_i}U-\frac{1}{2}U_{th}^T\frac{dK}{dx_i}U_{th}$$

Note that $\frac{dF}{dx_i}=\frac{dF_{th}}{dx_i}$ because the only design-dependent loads considered here are thermal, and the first two terms cancel yielding

$$\frac{d\hat{S}}{dx_i}=-\frac{1}{2}U^T\frac{dK}{dx_i}U+U_{th}^T\frac{dK}{dx_i}U-\frac{1}{2}U_{th}^T\frac{dK}{dx_i}U_{th} \tag{18}$$

which may be written as

$$\frac{d\hat{S}}{dx_i}=px_i^{p-1}(-\frac{1}{2}U_i^TK_iU_i+{U_{th}}_i^TK_iU-\frac{1}{2}U_{th_i}^TK_iU_{th_i}) \tag{19}$$

The above result is written in terms of the finite element matrices and the solutions from the thermal and mechanical finite element problems such that all terms on the right-hand side of Equations (15) and (19) are assumed known.

### 2.4 Alternative Convergence Criteria

The original optimality criterion algorithm was design for only negative design sensitivities. For purely mechanical systems, this is logical because increasing the density of any element can only make the part stiffer and thus decrease compliance. Once design-dependent thermal loads are included, the design sensitivities can be positive, which forces the update scheme to remove the maximum amount of material from those elements. To allow for the algorithm to operate, the sensitivities are shifted:

$$\frac{dC}{dx_i}\Big|_{new} = \begin{cases} \dfrac{dC}{dx_i} \quad , & \dfrac{dC}{dx_i} < 0 \\ \dfrac{dC}{dx_i} * \dfrac{\max\limits_{j}\left\{\frac{dC}{dx_j} \,\middle|\, \frac{dC}{dx_j} < 0\right\}}{\max\limits_{j}\left\{\frac{dC}{dx_j} \,\middle|\, \frac{dC}{dx_i} > 0\right\}} + \max\limits_{j}\left\{\frac{dC}{dx_j} \,\middle|\, \frac{dC}{dx_j} < 0\right\} & , \dfrac{dC}{dx_i} \geq 0 \end{cases} \tag{20}$$

This mapping preserves the ordering of the sensitivities and ensures that all sensitivities are negative, allowing the update scheme to operate properly. Other mappings exist that have these properties, and a comparison of different mapping methods will be done to determine how different mappings affect convergence rate and final structure.

Also, the structures generated do not always converge to a stable point. In some cases of strain energy optimization, the structure oscillates sinusoidally between two structures with a frequency of 150 iterations. When this occurred, the structure within the oscillation with a minimum optimization function value was selected as the final structure. Preliminary testing indicates that this oscillation may be due to singularities induced by the point load, but the existence of this cyclic behavior could indicate that either the tuning parameters need to be adjusted or a different update scheme should be used.

## 3. RESULTS

### 3.1 Test Description

The topology optimization method described above was applied to a series of problems assuming the following loading condition where we varied the ratio of thermal to mechanical loading. Each loading condition was optimized for strain energy and compliance separately, and the resulting structures were compared. The thermal boundary condition along the bottom edge of design domain, indicated by the blue region in Figure 1, is set to a temperature of 0ºC and a heat flux is applied to the top-right, denoted by the red arrow. The left edge is insulated, representing symmetry. A mechanical force of 500N is applied at the red arrow, and the bottom right corner is fixed in the y-direction. The left edge is fixed in the x-direction, representing symmetry. This design domain, illustrated in Figure 1, represents a bean in three-point bending, where we model only half the beam for simplicity.

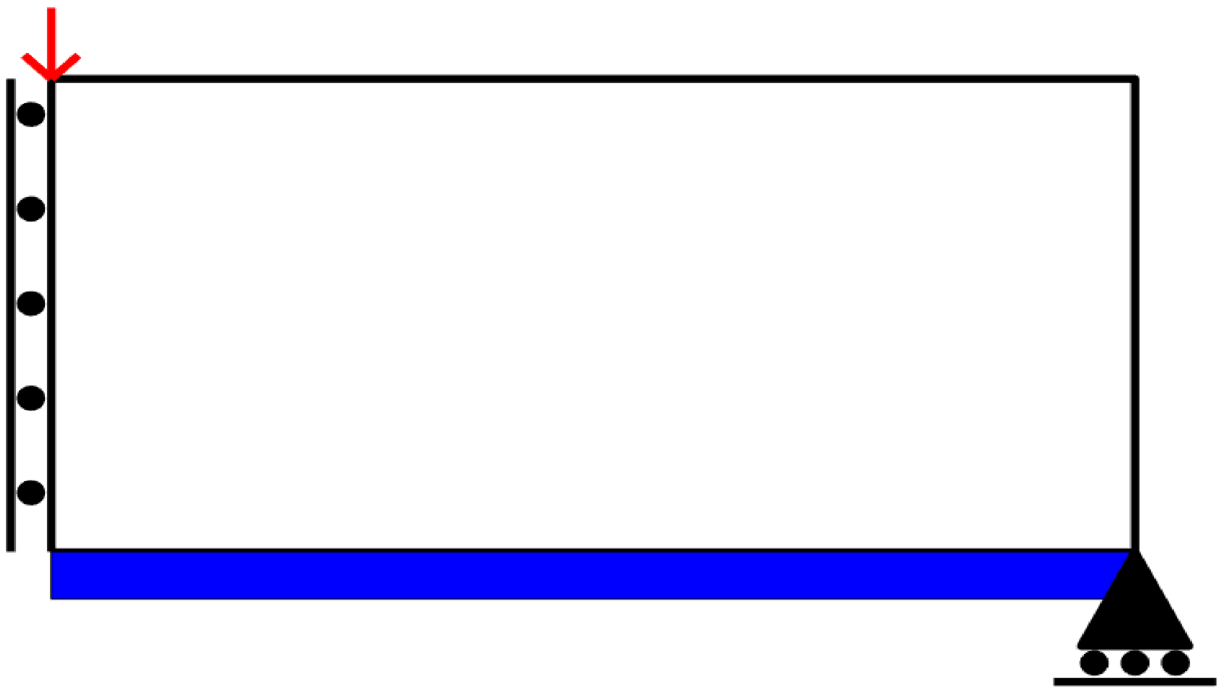

Figure 1: Design Domain

Six tests are conducted for different optimization functions and heat flux values.

| Test Number | Heat Flux (J) | Optimization Function |
|---|---|---|
| 1 | 5E-6 | Compliance |
| 2 | 5E-6 | Strain Energy |
| 3 | 1E-5 | Compliance |
| 4 | 1E-5 | Strain Energy |
| 5 | 3E-5 | Compliance |
| 6 | 3E-5 | Stain Energy |

Figure 2: Test Parameters

Each simulation is run for a penalty parameter of 3 for 1000 iterations. The domain is split into 100 by 200 elements, and the material is assumed to be 5 times stronger in the orientation direction than in the perpendicular direction.

# 4. CONCLUSIONS

## 4.1 Preliminary Results

The final structures are presented in Figure 2.

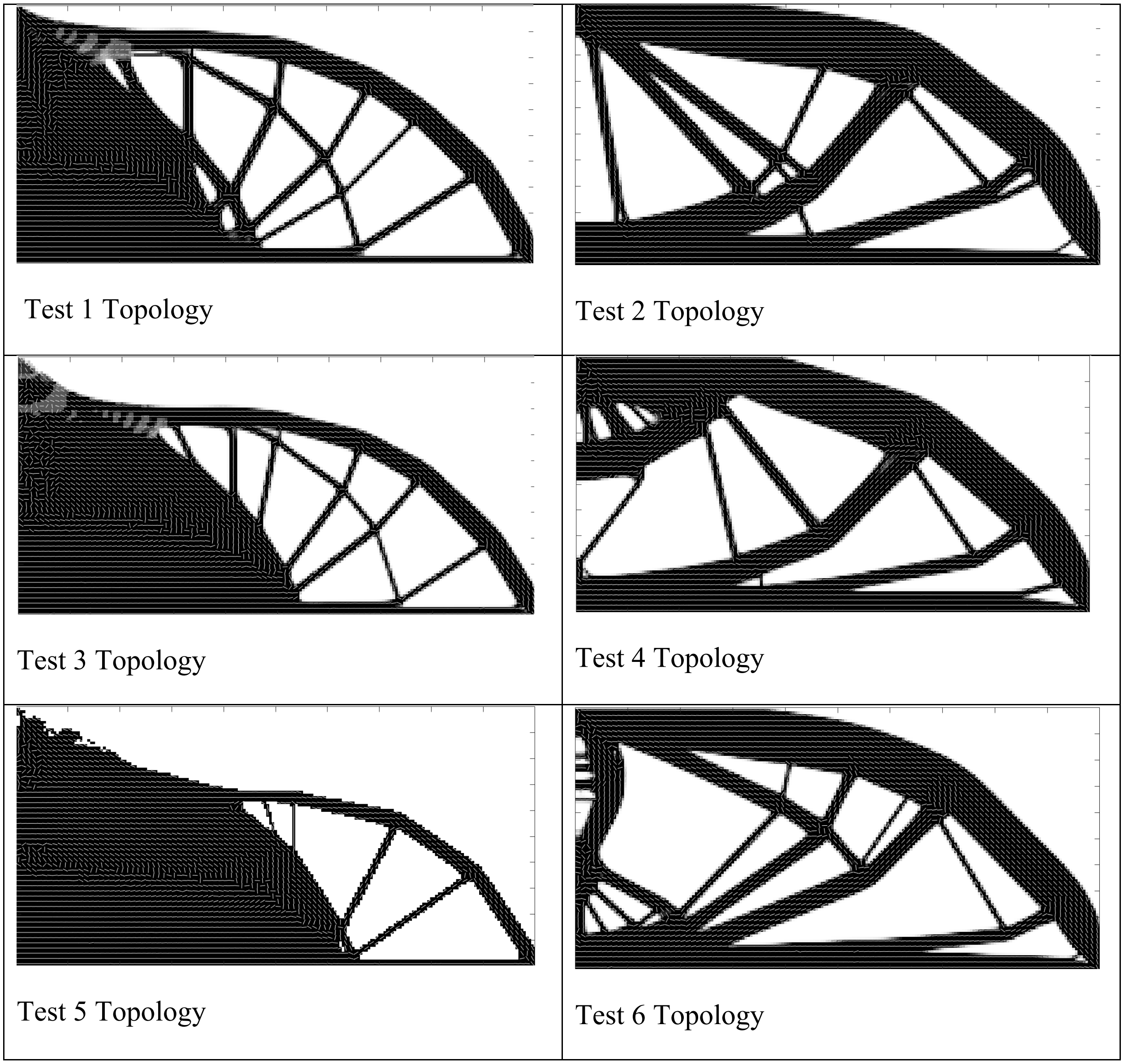


Figure 3: Final Optimization Result

These tests show the variation in the structure as thermal loads increase. In the case of zero thermal loads, strain energy and compliance are equal, and the topologies diverge as the heat flux increases.

## 4.2 Future Work

This adaptation of the optimality criterion method demonstrates preliminary success in optimizing the structure of a weakly coupled thermomechanical system. It can optimize either strain energy or compliance, but both present further challenges. Due to the mixed-sign compliance design sensitivities, a mapping must be used to ensure all sensitivities are negative while respecting the ordering. One such method has been implemented here, but other methods will be tested.

In strain energy simulations, particularly with high thermal loads, the structure can oscillate without converging. The tuning parameters may need to be adjusted, and alternate update schemes like the method of moving asymptotes may be necessary. These steps to ensure the robustness of the algorithm must be conducted before applying the algorithm to other systems.

The weakly coupled thermomechanical system considered here is a step toward accurately modeling the additive manufacturing process but does not fully represent it. Transient thermal three-dimensional systems will more accurately reflect the bead cooling process.

Although the system modeled her does not reflect the full complexity of additively manufactured structures, this method can be used to determine the topology of structures under steady-state thermal loading and mechanical loading. Systems such as automobile engine mounts, aircraft exhaust ducts, and internal combustion engine components could be optimized to minimize compliance or strain energy with this method.

# 5. REFERENCES


1. Bendsoe, Martin Philip, Kikuchi, Noboru. “Generating Optimal Topologies in Structural Design Using a Homogenization Method.” *Computer Methods in Applied Mechanics and Engineering* (1988): 197-224. DOI: 10.1016/0045-7825(88)90086-2
2. Svanberg, Krister. “The Method of Moving Asymptotes – a New Method for Structural Optimization.” *International Journal for Numerical Methods in Engineering* (1987): 359-373. doi:10.1002/nme.1620240207
3. Sigmund, O. “A 99 Line Topology Optimization Code Written in Matlab.” *Structural and Multidisciplinary Optimization* (2001): 120-127. DOI: 10.1007/s001580050176
4. Wang, Michael Yu, Wang, Xiaoming, Guo, Dongming. “A Level Set Method for Structural Topology Optimization.” *Computer Methods in Applied Mechanics and Engineering* (2003): 227-246. DOI: 10.1016/S0045-7825(02)00559-5
5. Bendsoe, M. P., Sigmund, O. *Topology Optimization Theory, Methods, and Applications*. Germany: Springer-Verlag Berlin Heidelberg 2003
6. Hoglund, Robert. “An Anisotropic Topology Optimization Method For Carbon Fiber-Reinforced Fused Filament Fabrication.” Masters Thesis, Baylor University.
7. Jiang, Dale. “Three Dimensional Topology Optimization with Orthotropic Material Orientation Design for Additive Manufacturing Structures.” Masters Thesis, Baylor University.
8. Jiang, Delin, Hoglund, Robert, Smith, Douglas E. “Continuous Fiber Angle Topology Optimization for Polymer Composite Deposition Additive Manufacturing Applications.” *Fibers* (2019): DOI: 10.3390/fib7020014

9. Luo, J. H., Gea, H. C. "Optimal Orientation of Orthotropic Materials Using an Energy Based Method." *Structural Optimization* (1998): 230-236. DOI: 10.1007/BF01203536

10. Deaton, Joshua. "Design of Thermal Structures Using Topology Optimization." Dissertation for Doctor of Philosophy, Wright State University 2009.

11. Pederson, Pauli, Pederson, Niels. "Strength Optimized Designs of Thermoelastic Structures." *Structural and Multidisciplinary Optimization* (2010): 681-691. DOI: 10.1007/s00158-010-0535-5

12. Zhang, Weihong, Yang, Jungang, Xu, Yingjie, Gao, Tong. "Topology Optimization of Thermoelastic Structures: Mean Compliance Minimization or Elastic Strain Energy Minimization." *Structural and Multidisciplinary Optimization* (2014): 417-429. DOI: 10.1007/s00158-013-0991-9

13. Neiford, David John, Grandhi, Ramana V., Deaton, Joshua D., Beran, Philip S. "Level-Set Topology Optimization of Thermoelastic Structures – a Comparison of Compliance, Strain Energy, and Stress Objectives." *2018 Multidisciplinary Analysis and Optimization Conference*. Atlanta, Georgia, June 25-29 2018. AIAA Aviation Forum. DOI: 10 2514/6 2018-3577

14. Kunc, Vlastimil, Compton, Brett, Simunovic, Srdjan, Duty, Chad, Love, Lonnie, Post, Brian, Blue, Craig, Talagani, Farid, Dutton, Renly, Godines, Cody, DorMohammadi, Saber, Baid, Harsh, Abdi, Frank. "Modeling of Large Scale Reinforced Polymer Additive Manufacturing." *ANTEC*. Orlando, Florida, March 23-25 2015. Society of Plastics Engineers.

15. Compton, Brett G., Post, Brian K., Duty, Chad E., Love, Lonnie, Kunc, Vlastimil. "Thermal Analysis of Additive Manufacturing of Large-Scale Thermoplastic Polymer Composites." *Additive Manufacturing* (2017): 77-86. DOI: 10.1016/j.addma.2017.07.006